An Advanced General Dominant Eigenvalue Method of Accelerating Successive Substitution during Flash Calculation for Compositional Reservoir Model

Xiaoman Wang, Dengfeng Wei, Xiaohong Wang, Xisen Zhao, Jian Li, Benoît Noetinger

HAL Id: hal-03695410
https://ifp.hal.science/hal-03695410

Submitted on 14 Jun 2022

Original article

An advanced general dominant eigenvalue method of accelerating successive substitution during flash calculation for compositional reservoir model

Xiaoman Wang[1], Dengfeng Wei[2], Xiaohong Wang[1]⊙*, Xisen Zhao[2], Jian Li[2], Benoît Noetinger[3]

[1]*Department of Thermal Science and Energy Engineering, University of Science and Technology of China, Hefei 230026, P. R. China*
[2]*Shaanxi Yanchang Petroleum (Group) Co. Ltd., Xi'an 710065, P. R. China*
[3]*IFP Energies nouvelles, 1-4 avenue de Bois-Préau, Paris, 92852 Rueil-Malmaison, France*

Abstract:
The efficiency and accuracy of phase equilibrium calculations are essential in compositional reservoir models. Usually, a significant part of the computational effort in compositional reservoir simulations is spent on phase equilibrium calculations. The nonlinear nature of phase equilibrium calculations requires an iterative solution procedure. Although the successive substitution method (SSM) is robust and simple to implement, it suffers from slow convergence, especially near the critical point of the mixture. The general dominant eigenvalue method (GDEM) has been widely used to accelerate SSM, but its stability and efficiency deteriorate as the temperature and pressure approach the critical point. This paper proposes a modified form of GDEM to improve its performance in the near-critical region. The modifications have two aspects. First, the liquid phase fraction in the mixture is added as a variable when performing GDEM acceleration, improving both stability and efficiency. The second modification is a post-calibration step imposed to replace the conventional criterion, which is applied before triggering GDEM. With the help of the post-calibration step, the stability of the modified GDEM is ensured, and more importantly, the calculation efficiency can be improved. Numerical tests of three hydrocarbon mixtures, including different numbers of components, show that the stability of the modified GDEM is almost the same as SSM and that its calculation efficiency is much higher than SSM and the conventional GDEM.

1. Introduction

CO$_2$-enhanced oil recovery (CO$_2$-EOR) is an effective CO$_2$ capture, utilization, and storage technique to reduce greenhouse gases in the atmosphere and achieve carbon neutrality goals (Soeder, 2021; Xu et al., 2022). The numerical simulations for CO$_2$-EOR can provide accurate predictions of multiphase flows and phase states in the reservoir, with significant scientific and practical value. Usually, a compositional reservoir model is used for CO$_2$-EOR numerical simulations (Afanasyev et al., 2021). The formulations of CO$_2$-EOR compositional models fall primarily into two groups. One group includes the primary variables of saturation, individual phase composition, and pressure. The other is based on the mole, mass, or overall fractions and pressure. Both formulations are strongly coupled systems, which contain a large number of nonlinear partial differential equations. The fluid components in the reservoir are complex and the solution scale is large. Therefore, developing an efficient solution algorithm is a principal focus of research. When solving primary variables, fully implicit methods (Coats, 1980), adaptive implicit methods (Moortgat, 2017), sequential methods (Hu et al., 2020; Moncorgé et al., 2020), and other methods (Coats, 2000; Mostafavi et al., 2020) have all been studied and tested for their convergence and efficiency. In addition to algorithm

research, parallel processing techniques (Lian et al., 2019) and graphics processing units can also be used to improve the calculation speed for the compositional model of CO_2 flooding.

Besides the calculations for primary variables, phase equilibrium calculations are another crucial part of the compositional reservoir simulations. As the basic procedure for solving secondary variables in compositional reservoir models, phase equilibrium calculations refer to solving nonlinear equations to obtain phase compositions under a given temperature and pressure. In simulations, phase equilibrium calculations solve a coupled set of nonlinear equations in each grid block at every time step (Haugen and Beckner, 2013). Finding a solution may consume more than 75% of the total computational effort (Nichita and Leibovici, 2013). Furthermore, failures in phase equilibrium calculations can affect simulation results significantly and cause non-convergence in the simulation (Petitfrere and Nichita, 2015). Thus, fast and robust flash algorithms are essential for simulating multi-compositional flows in petroleum reservoirs.

Phase equilibrium calculations are composed of two steps (Li, 2021). The first is the stability analysis derived from Gibbs free energy and it is used to judge whether the feed is stable in the single-phase state. The second is the phase-split calculation, also called the flash calculation, which is carried out if the feed is unstable. The nonlinear nature of flash calculation requires iterative solution procedures. These iterative procedures can be divided into three major groups: the conventional successive substitution method (SSM) and its acceleration algorithms, Newton-Raphson methods (Michelsen, 1982b; Zhu et al., 2018; Wang et al., 2021), and reduced-variables methods (Michelsen, 1986; Pan and Firoozabadi, 2003; Li and Johns, 2006; Nichita and Graciaa, 2011; Zhao et al., 2020).

To the best of our knowledge, existing algorithms have several disadvantages and still need to be improved to meet the requirements for use in engineering. For example, using Newton-Raphson methods can be challenging since their Jacobian matrices tend to be singular and lead to divergence in the near-critical region. The acceleration effects of reduced-variables methods are questioned. There is some controversy exists, so no definite conclusion has been made about whether reduced-variables methods are more efficient than conventional ones (Michelsen et al., 2013; Gorucu and Johns, 2015; Petitfrere and Nichita, 2015). The test results of Michelsen et al. (2013) indicate that reduced-variables methods are faster only for a large number of components and the speedup is modest (less than 20%). Notably, when the temperature and pressure are close to the critical point of the components, the nonlinearity of the equations solved by the flash calculation is enhanced. Flash calculations in this region are not only slow but also prone to divergence. Both Newton-Raphson and reduced-variables methods have high failure rates (Gorucu and Johns, 2015).

SSM is more robust and simpler to implement than the Newton-Raphson and reduced-variables methods. However, SSM suffers from a slow convergence speed when pressure and temperature are close to the phase boundary near the critical point (Li and Firoozabadi, 2012). Some numerical algorithms can be approached to linearly accelerate the convergence process of SSM, including dominant eigenvalue method (DEM) (Orbach and Crowe, 1971), general dominant eigenvalue method (GDEM) (Crowe and Nishio, 1975), and accelerated successive substitution (Mehra et al., 1983) et al. Among various linear-acceleration methods, GDEM acceleration provides a linear approximation to iteration results obtained after a large number of iterations using SSM and has been widely used. In 1958, Wegstein (1958) proposed a linear relation, accelerating the convergence of the single variable problem using the iterative values to approximate a predicted value. Orbach and Crowe (1971) pointed out that this type of linear relationship proposed by Wegstein could be approximated by a geometric sequence while the convergence process is determined by the dominant eigenvalue of the matrix, which is composed of the common ratios among variables. They proposed DEM to accelerate the convergence process using dominant eigenvalue and previous iteration values for prediction. Belkadi et al. (2013) employed DEM as a part of an efficient implementation of phase equilibrium calculations. Crowe and Nishio (1975) proposed GDEM, which allows for selecting multiple eigenvalues when predicting the iteration values, meaning that iteration values in previous multiple steps can be used. Soliman (1981, 1985) presented an alternative derivation for GDEM and improved its convergence. Ordinarily, the iteration variables in GDEM for flash calculations are phase equilibrium ratios. Gupta et al. (1988) studied the application of DEM and GDEM using the mole fraction of gas and liquid components as iteration variables. Zhao et al. (2020) recently applied the GDEM acceleration to the reduced-SSM, which also showed the efficiency of GDEM.

Current versions of the GDEM algorithm still face challenges. When the temperature and pressure approach the critical point, there is a certain gap between GDEM and SSM in success rate (Zhao et al., 2020). Michelsen (1993) stated that GDEM frequently "over-extrapolates" in the near-critical region, which causes the flash calculations to fail. Li and Firoozabadi (2012) pointed out that GDEM may cause calculations to converge more slowly and even diverge when temperature and pressure near the critical point of the mixture. In the near-critical region, slight changes in the component equilibrium ratio seriously impact the solution of the gas-liquid fraction. If the predicted value of the equilibrium ratio calculated from GDEM is not accurate enough, the convergence of the flash calculation will be damaged. In the compositional numerical simulation of CO_2 flooding, flash calculations in the near-critical region often occur. Therefore, it is necessary to improve the robustness and efficiency of GDEM, especially in the near-critical region.

This study modified the conventional GDEM to improve its performance near the critical region in two respects. First, the liquid fraction is added as a variable when performing GDEM, improving its stability and speed. Second, the conventional criterion before triggering GDEM is abandoned. Instead, a post-calibration step is imposed after each GDEM acceleration to ensure stability. Abandoning the conventional criterion can significantly improve the calculation efficiency of the modified

GDEM.

2. Theoretical models

2.1 Flash calculation

Classic phase equilibrium calculations have two steps: a stability test to judge whether the mixture is stable at the given temperature and pressure, and a flash calculation to calculate the phase fractions and phase compositions if the mixture is unstable. Details of the stability analysis can be found in Michelsen (1982a). In this section, the procedure of the flash calculation is briefly introduced.

Flash calculations need to solve equations derived from component fugacity equilibrium and mass conservation. The equilibrium criterion can be written as:

$$\ln f_i^L - \ln f_i^V = \ln y_i \varphi_i^V - \ln x_i \varphi_i^L = 0 \qquad (1)$$

where f_i is the fugacity of component i; the superscripts L and V represent the liquid and gas phase respectively, while the variables x_i and y_i represent the liquid and gas phase mole fractions of component i, respectively. φ_i is the fugacity coefficient of component i, which can be calculated by implementing equations of state (EOS) such as SRK-EOS (Soave, 1972), PR-EOS (Peng and Robinson, 1976), etc. In this study, PR-EOS is employed in both the stability test and flash calculation.

When introducing the vector of equilibrium ratios $\mathbf{K}=\{K_i,...,K_{Nc}\}$ with:

$$K_i = \frac{y_i}{x_i} \qquad (2)$$

and from the mass conservation relation $x_i F_L + y_i F_v = z_i$ with z_i always given, one can obtain:

$$x_i = \frac{z_i}{F_L + (1 - F_L)K_i}, \quad y_i = x_i K_i \qquad (3)$$

where F_L represents the liquid phase fraction, F_v represents the vapor phase fraction, and z_i represents the toltal mole fraction of component i. Mass conservation can also be represented as the nonlinear Rachford–Rice (Rachford and Rice, 1952) equation:

$$\sum_{i=1}^{N}(x_i - y_i) = \sum_{i=1}^{N} \frac{z_i(1 - K_i)}{F_L + (1 - F_L)K_i} = 0 \qquad (4)$$

The fugacity coefficients for evaluating K-values are obtained from the PR-EOS (Peng and Robinson, 1976), which is expressed as:

$$P = \frac{RT}{V - b_m} - \frac{a_m}{V(V + b_m) + b_m(V - b_m)} \qquad (5)$$

where P represents the pressure, T represents the temperature, and V represents the mole volume of the mixture. The van der Waals mixing rule is used for parameters a_m and b_m:

$$a_m = \sum_{i=1}^{Nc}\sum_{j=1}^{Nc} x_i x_j a_{ij}, \quad b_m = \sum_{i=1}^{Nc} x_i b_i \qquad (6)$$

with:

$$a_{ij} = (1 - k_{ij})(a_i a_j)^{0.5},$$

$$a_i = 0.45724 \frac{R^2 T_{ci}^2}{P_{ci}} \left[1 + m_i \left(1 - \frac{T^{0.5}}{T_{ci}^{0.5}}\right)\right]^2,$$

$$m_i = 0.37464 + 1.54226\omega_i - 0.26992\omega_i^2,$$

$$b_i = 0.07780\frac{RT_{ci}}{P_{ci}}.$$

In the above equations, N_c is the number of components; R is the gas constant; T_{ci} and P_{ci} are the critical temperature and pressure of component i; ω_i is the acentric factor of component i; and k_{ij} is the binary interaction parameter between components i and j; a_{ij}, a_i, b_i, and m_i are all parameters of PR-EOS.

Introducing the compressibility factor, $Z = PV/RT$, Eq. (5) can be rewritten as:

$$Z^3 - (1 - B)Z^2 + (A - 2B - 3B^2)Z - (AB - B^2 - B^3) = 0 \quad (7)$$

where the parameter A and B are represented as:

$$A = \frac{a_m P}{R^2 T^2}, \quad B = \frac{b_m P}{RT} \qquad (8)$$

The fugacity coefficient of component i can be calculated from the following equation:

$$\ln \varphi_i = \frac{b_i}{b_m}(Z - 1) - \ln(Z - B)$$
$$- \frac{A}{2\sqrt{2}B}\left(\frac{2}{a_m}\sum_{j=1}^{Nc} x_j a_{ij} - \frac{b_i}{b_m}\right)\ln\frac{Z + 2.414B}{Z - 0.414B} \qquad (9)$$

Notice that the PR-EOS Eq. (5) is suitable for both the vapor and liquid phases. For the liquid phase, the minimum real root of the cubic equation Eq. (7) is selected. For the vapor phase, where the liquid mole fractions x_i in the above relations should be replaced by the vapor mole fractions y_i, the maximum real root of the cubic equation Eq. (7) is selected.

In solving the complete set of nonlinear equations, Eqs. (1)-(9), mole fractions x_i, y_i, the liquid phase fraction F_L and the phase equilibrium ratios $\mathbf{K}=\{K_1,...,K_{Nc}\}$ can be calculated. Iterative methods, such as SSM, Newton-Raphson methods, or others must be employed to solve this set of equations due to its nonlinear nature.

2.2 SSM

Using SSM to solve the flash calculation problem has the advantage of easy implementation and high stability. The SSM procedure, which is the basis of GDEM, is briefly summarized as follows:

Step 1: Start with phase stability test results to obtain the initial guess of the phase equilibrium ratio $\mathbf{K}^{(0)}$.

Step 2: Denote the current iteration value of phase equilibrium ratio as $\mathbf{K}^{(n)}$ with denoting the iteration step. Calculate the liquid phase fraction F_L by solving Eq. (4) with the Newton-Raphson method or others.

Step 3: Substitute the fluid phase fraction F_L into Eq. (3) to calculate mole fractions x_i and y_i.

Step 4: Use the EOS (PR-EOS is employed here) to calculate fugacity coefficients φ_i^L and φ_i^V for the liquid and the vapor phases, respectively.

Step 5: Check whether the fugacity equilibrium relation Eq. (1) is satisfied. If not, the phase equilibrium ratios are updated as $K_i^{(n+1)} = \varphi_i^L / \varphi_i^V$, and **Steps 2-5** are repeated until fugacity equilibrium Eq. (1) is achieved. Then the current iteration values of x_i, y_i, F_L, and K_i are the results of the flash calculation.

2.3 GDEM

When the flash calculation is performed in the near-critical region or around the phase envelope, SSM is quite time-consuming. Michelsen (1982b) suggested using GDEM to accelerate SSM. Conventionally, the phase equilibrium ratios have been used as iteration variables, and their variations between two iterations can be approximated by a linear difference equation after enough iterations:

$$\Delta \mathbf{K}^{(n+1)} = \mathbf{A} \cdot \Delta \mathbf{K}^{(n)} \qquad (10)$$

where $\Delta \mathbf{K}^{(n)} = \mathbf{K}^{(n+1)} - \mathbf{K}^{(n)}$ and $\mathbf{A}$ is a $N_c \times N_c$ matrix. According to the Cayley-Hamilton theorem, the characteristic equation of matrix $\mathbf{A}$ can be transformed as:

$$|\lambda \mathbf{I} - \mathbf{A}| = \sum_{j=0}^{m} \mu_j \lambda^{m-j} \qquad (11)$$

where m represents the rank of matrix $\mathbf{A}$, $\mathbf{I}$ is a identity matrix. Denote the root of the characteristic equation Eq. (11) as λ_j ($j = 1, ..., m$), which are eigenvalues of matrix $\mathbf{A}$. The corresponding eigencoefficients μ_j are defined as:

$$\mu_0 = 1, \quad \mu_j = (-1)^j \sum \lambda_{i_1} \lambda_{i_2} \lambda_{i_3} ... \lambda_{i_j}$$
$$(1 \leqslant j \leqslant m; 1 \leqslant i_1 \leqslant i_2 ... \leqslant i_j \leqslant m) \qquad (12)$$

From the Cayley-Hamilton theorem, matrix $\mathbf{A}$ satisfies the following relation:

$$\sum_{j=0}^{m} \mu_j \mathbf{A}^{m-j} \Delta \mathbf{K}^{(n-m)} = \mathbf{0}, \quad n \geqslant m \qquad (13)$$

Thus, applying Eq. (10) repeatedly, one can obtain:

$$\sum_{j=0}^{m} \mu_j \Delta \mathbf{K}^{(n-j)} = \mathbf{0}, \quad n \geqslant m \qquad (14)$$

Suppose all eigenvalues λ_j are distinct and denote the eigenvector belonging to the eigenvalue λ_j as $\mathbf{v}_j$. From Eq. (10), one can obtain:

$$\Delta \mathbf{K}^{(n)} = \mathbf{A}^n \cdot \Delta \mathbf{K}^{(0)} = \sum_{j=1}^{m} \mathbf{v}_j \lambda_j^n \qquad (15)$$

with $\Delta \mathbf{K}^{(0)} = \sum_{j=1}^{m} \mathbf{v}_j$.

Eq. (15) indicates that the eigenvalues λ_j determine the convergence of SSM. Label λ_j in descending order of absolute magnitude and suppose that only the first k of them $\{\lambda_j | j = 1, ..., k < m\}$ are large enough to dominate the iteration. In this sense, the iteration behaves as if $\lambda_j = 0$ ($j > k$). According to the definition Eq. (11) of the eigencoefficients, each eigencoefficient u_j ($j > k$) contains at least one λ_l ($l > k$). Thus, each eigencoefficient $u_j = 0$ ($j > k$), and correspondingly, Eq. (14) can be approximated as:

$$\sum_{j=0}^{k} \hat{\mu}_j \Delta \mathbf{K}^{(n-j)} = \mathbf{0}, (k \leqslant m, n \geqslant m) \qquad (16)$$

where $\hat{\mu}_j$ are estimates of μ_j by treating $\lambda_j = 0$ ($j > k$). Obviously, the approximation is much more accurate with a larger value of the parameter k. In this paper, $k = 3$. The value of $\hat{\mu}_j$ ($j = 0, 1..., k$) can be obtained by solving the linear equation:

$$\sum_{j=0}^{k} \hat{\mu}_j b_{jw} = 0, (w = 1, 2, ..., k) \qquad (17)$$

with $b_{jw} = \langle \Delta \mathbf{K}^{(n-j)}, \Delta \mathbf{K}^{(n-w)} \rangle$.

With the help of Eq. (16), the final result $\mathbf{K}^{(\infty)}$ predicted from Eq. (10) can be approximated as:

$$\hat{\mathbf{K}}^{(\infty)} = \mathbf{K}^{(n+1)} - \frac{\sum_{i=0}^{k-1} (\sum_{j=i+1}^{k} \hat{\mu}_j) \Delta \mathbf{K}^{(n-i)}}{\sum_{j=0}^{k} \hat{\mu}_j} \qquad (18)$$

One can directly substitute $\hat{\mathbf{K}}^{(\infty)}$ into the next iteration step to accelerate the convergent procedure. Details of GDEM are well recorded by Crowe and Nishio (1975) and Zhao et al. (2020).

The criterion of GDEM is essential to its robustness and efficiency. In 2020, Zhao et al. (2020) used the ratio of $\|\Delta \mathbf{K}^{(n)}\|$ and $\|\mathbf{K}^{(n)}\|$ as the criterion to trigger GDEM:

$$\frac{\|\Delta \mathbf{K}^{(n)}\|}{\|\mathbf{K}^{(n)}\|} < \varepsilon \qquad (19)$$

where ε is a user-defined small value which could be 10^{-3}, 10^{-4}, and 10^{-5}, et al. When the criterion Eq. (19) is satisfied, the acceleration process of GDEM is triggered, and the calculated value $\hat{\mathbf{K}}^{(\infty)}$ from Eq. (18) will be used in the next iteration. According to the criterion Eq. (19), the value of ε determines when to use GDEM to accelerate the iteration process. The conservative choice with small ε does not notably improve the calculation efficiency. On the contrary, a large ε can improve the calculation efficiency greatly but does harm to the stability.

3. Modification of GDEM

3.1 Adding the fluid phase fraction F_L as a variable in GDEM

Flash calculation requires solving $N_c + 1$ unknowns which are the phase equilibrium ratios K_i ($i = 1, 2, ..., N_c$) of each component and the liquid phase fraction F_L (or the vapor phase fraction F_V). In the conventional GDEM as described above, only N_c unknowns, the phase equilibrium ratios K_i, are considered when performing GDEM. The other variable F_L is updated independently by Eq. (4) from the current values of K_i. As temperature and pressure approach the critical point of the mixture, the phase equilibrium ratios K_i will approach 1 for each component i. From Eq. (4), one can obtain:

$$\frac{\partial F_L}{\partial K_i} = \frac{-z_i}{[F_L + (1 - F_L)K_i]^2 \sum_{j \neq i}^{N_c} \frac{z_i(1-K_j)^2}{[F_L+(1-F_L)K_j]^2} + (K_i - 1)^2 z_i} \qquad (20)$$

It can be seen from Eq. (20) that $\partial F_L/\partial K_i$ approaches infinity as all K_i approach 1, which means that a slight change in K_i will cause a drastic change in F_L. Even if K_i converge, F_L may still have a significant error. Thus, choosing only K_i as iterative variables to perform GDEM may not be appropriate.

In the modified GDEM, the iterative values of the liquid phase fraction F_L are added to the variables to construct the acceleration algorithm. As a result, the new augmented variable $\mathbf{D}$ can be defined as:

$$\mathbf{D} = (K_1, K_2, .., K_{N_c}, F_L)^T \qquad (21)$$

Correspondingly, the linear difference equation between two iterations can be approximated by:

$$\Delta \mathbf{D}^{(n+1)} = \mathbf{A}' \cdot \Delta \mathbf{D}^{(n)} \qquad (22)$$

Denote the eigencoefficients of the augmented iterative matrix $\mathbf{A}'$ as μ_j'. Their estimates μ_j' $(j = 0, 1, ..., k)$ can be calculated following the process described above. Similar to Eq. (18), the final results $\mathbf{D}^{(\infty)}$ for the next iteration step after GDEM can be approximated as:

$$\hat{\mathbf{D}}^{(\infty)} = \mathbf{D}^{(n+1)} - \frac{\sum\limits_{i=0}^{k-1}\left(\sum\limits_{j=i+1}^{k} \hat{\mu}_j'\right) \Delta \mathbf{D}^{(n-i)}}{\sum\limits_{j=0}^{k} \hat{\mu}_j'} \qquad (23)$$

Compared to the conventional GDEM, the difference in the modified GDEM is that the augmented matrix $\mathbf{A}'$, which contains iterative information of the liquid phase fraction F_L, is employed to replace the original iterative matrix $\mathbf{A}$. The dominant eigenvalues of the augmented matrix $\mathbf{A}'$ are different from those of the matrix $\mathbf{A}$, especially near the critical region. Thus, the calculated values of $\hat{\mu}_j'$ are different from the values of $\hat{\mu}_j'$ by the conventional GDEM. Through this method, the predicted values of K_i in the modified GDEM are different from those predicted by the conventional GDEM. From the application point of view, the stability of the modified GDEM, which takes the iterative behavior of the liquid phase fraction F_L into consideration, is improved.

3.2 Modified criterion for GDEM

As mentioned in Section 2.3, the criterion Eq. (19) is employed to trigger the acceleration process in the conventional GDEM. Generally speaking, the criterion Eq. (19) can only be satisfied after enough number of SSM iterations. In other words, before GDEM is triggered, many SSM iterations have already been performed. In fact, as described in Section 2.3, so long as $k+1$ terms $\{\Delta \mathbf{K}^{(n-j)} | j = 0, ..., k\}$ are obtained after completing $k+1$ successive SSM iterations, the acceleration process of GDEM can be implemented. If the original criterion Eq. (19) is abandoned and GDEM is implemented immediately after $k+1$ steps of SSM iterations, the total efficiency will be improved greatly. Based on this idea, a modified form of GDEM is proposed, in which a much higher efficiency can be achieved by triggering GDEM immediately after $k+1$ SSM iterations.

If the predicted values obtained after GDEM acceleration

are used directly in the subsequent iteration, especially when the criterion Eq. (19) is abandoned, the iterative process is usually unstable because not all $\hat{K}_i^{(\infty)}$ of the predicted $\hat{\mathbf{K}}^{(\infty)}$ keep the right direction of convergence. Even if the criterion Eq. (19) is employed, the correct direction of convergence cannot be ensured for each component since not all of the eigenvalues of the iterative matrix are considered in GDEM.

To ensure the iterative direction for each component K_i after GDEM in accordance with SSM, a post-calibration step is added to the GDEM procedure. After GDEM acceleration, the predicted value $\hat{\mathbf{K}}^{(\infty)}$ (or $\hat{\mathbf{D}}^{(\infty)}$ in its modified form) is not directly employed in the next iterative step. Instead, the iterative direction of each component in $\hat{\mathbf{K}}^{(\infty)}$ (or $\hat{\mathbf{D}}^{(\infty)}$) is examined. Those components $\hat{K}_i^{(\infty)}$ (or $\hat{D}_i^{(\infty)}$) with their iterative direction in accordance with SSM are retained, and the others are replaced by their iterative value $K_i^{(n+1)}$ (or $D_i^{(n+1)}$) in SSM.

In practical application, it is found that using the predicted value $\hat{K}_i^{(\infty)}$ from GDEM may cause divergence if $\Delta K_i^{(n_{GDEM})}$ (defined as $\Delta K_i^{(n_{GDEM})} = \hat{K}_i^{(\infty)} - K_i^{(n)}$) differs significantly from $\Delta K_i^{(n)}$. To alleviate this problem, the predicted value $\hat{K}_i^{(\infty)}$ should also be abandoned and replaced by $K_i^{(n+1)}$ if the ratio $|\Delta K_i^{(n_{GDEM})}/\Delta K_i^{(n)}|$ is too large.

According to the above considerations, a post-calibration step is imposed after each GDEM acceleration to judge whether the predicted value $\hat{K}_i^{(\infty)}$ will be used in the next iteration. The post-calibration step (in the form of augmented variables $\mathbf{D}$) can be described as follows:

$$D_i^{[n+1]} = \begin{cases} D_i^{(n+1)}, & \text{sgn}(\tau_i) < 0 \quad \text{or} \quad |\tau_i| > \tau_c \\ \hat{D}_i^{(\infty)}, & \text{sgn}(\tau_i) \geq 0 \quad \text{and} \quad |\tau_i| \leq \tau_c \end{cases} \qquad (24)$$

with:

$$\tau_i = \frac{\Delta D_i^{(n_{GDEM})}}{\Delta D_i^{(n)}},$$

$$\Delta D_i^{(n_{GDEM})} = \hat{D}_i^{(\infty)} - D_i^{(n)},$$

$$\Delta D_i^{(n)} = \Delta D_i^{(n+1)} - D_i^{(n)}.$$

The parameter τ_c in the post-calibration step Eq. (24) is a user-defined constant, and our numerical tests suggest that it be set to $\tau_c = 10^4$. The calibrated value $D_i^{[n+1]}$ will be employed in the next iteration. After calibration, each component D_i remains in the same iterative direction as in SSM, and the ratio $|\Delta D_i^{[n+1]}/\Delta D_i^{(n)}|$ (with $\Delta D_i^{[n+1]} = D_i^{[n+1]} - D_i^{(n)}$) is restricted. This ensures the stability of the entire iterative process.

Since the conventional criterion Eq. (19) is abandoned and replaced by the post-calibration step Eq. (24), the GDEM acceleration process will be triggered immediately after $k+1$ SSM iterations. Thus, the overall iterative efficiency of the modified GDEM is greatly improved.
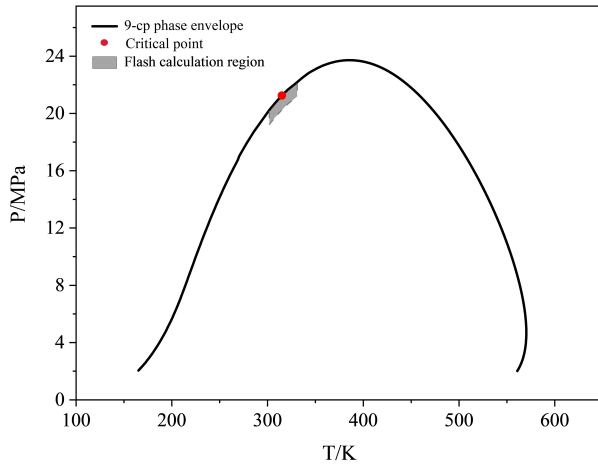
3.3 Steps of the modified GDEM

The steps of the modified GDEM are briefly described as follows.

Step 1: Start with phase stability test results and obtain the

Table 1. Flash calculation results of the 9-cp mixture.

Algorithm	Failure rate (%)	Average iterative steps	Average CPU time (s)
SSM	0.00	3,129	2.75×10^{-3}
Conventional GDEM (with $\varepsilon = 1.0 \times 10^{-3}$)	36.81	-	-
Conventional GDEM (with $\varepsilon = 1.0 \times 10^{-4}$)	27.95	-	-
Conventional GDEM (with $\varepsilon = 1.0 \times 10^{-5}$)	14.17	2,648	2.52×10^{-3}
Modified GDEM	0.90	168	1.95×10^{-4}

Fig. 1. Illustration of the phase envelope and the test region for the 9-cp mixture.

initial guess of the phase equilibrium ratios $\mathbf{K}^{(0)}$.

Step 2: Follow the standard steps in SSM to obtain $k + 1$ iterative values of the phase equilibrium ratio and the liquid phase fraction $\{\mathbf{D}^{(n-j+1)} | j = 0, 1, ...k\}$ (see Section 2.2).

Step 3: Perform the modified GDEM procedure to obtain the predictive value $\hat{\mathbf{D}}^{(\infty)}$ according to Eq. (23). (The iterative values of the liquid phase fraction $\{F_L^{(n-j+1)} | j = 0, 1, ...k\}$ are added as variables in GDEM, which can improve the stability of the entire iterative process.)

Step 4: Update the iterative value $D_i^{[n+1]}$ for the next iteration according to the post-calibration step Eq. (24).

Step 5: Check whether the fugacity equilibrium relation is satisfied. If not, update the phase equilibrium ratios $\mathbf{K}$ according to the fugacity equality and repeat **Steps 2-5** until fugacity equality is achieved. Then, the current iteration values of K_i, F_L, x_i, and y_i are the solutions of the flash calculation.

4. Numerical tests

This section reports the high performance of the modified GDEM during flash calculations in the near-critical region indicated through numerical tests. Three hydrocarbon mixtures with different components are employed to perform flash calculations. For comparison, the test results of SSM and the conventional GDEM are also provided. The initial guesses of phase equilibrium ratios in all of the tests are obtained through phase-stability analysis proposed by Michelsen (1982a). The convergence criterion is set as the residual of fugacity equality relation $\left\| x_i \varphi_i^L - y_i \varphi_i^V \right\|_\infty < 10^{-10}$. A flash calculation is marked as failed if a trivial solution is obtained, the Rachford-Rice equation breaks down, the liquid phase fraction exceeds its bounds during iterations, or the number of iterations exceeds 12,000.
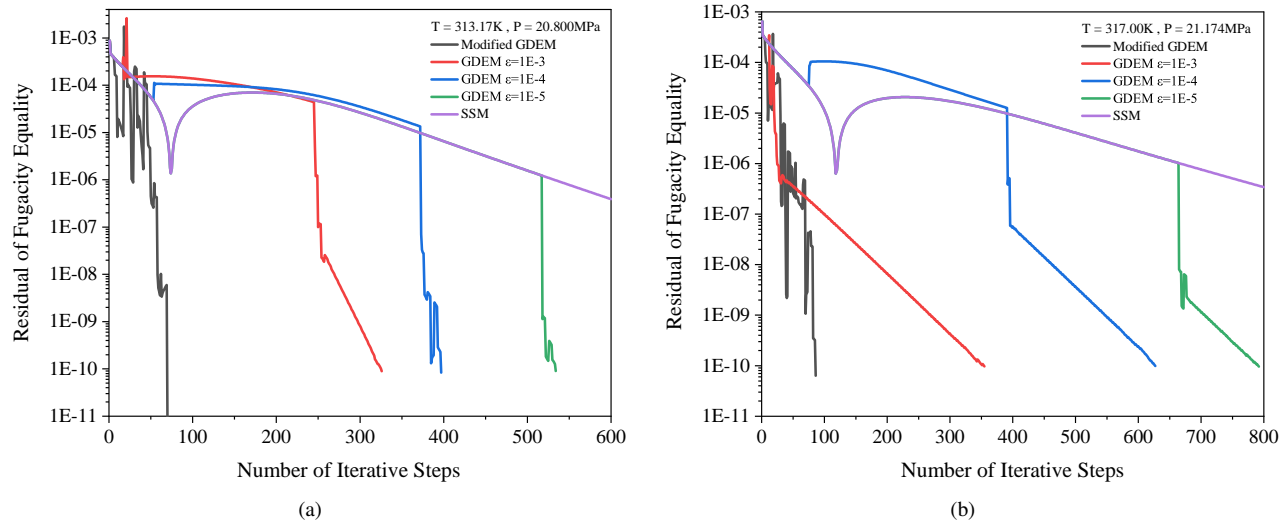
4.1 Test for the 9-component mixture

The 9-component mixture comprises CO_2, N_2, and 7 other hydrocarbons. Fluid compositions and EOS parameters of the 9-component mixture can be found in Kenyon (1987). Its critical temperature and pressure are $T_c = 315.37$ K and $P_c = 21.55$ MPa, respectively. Fig. 1 shows the phase envelope and the critical point of this mixture. The test region is a curved quadrilateral ([300 K, 330 K]$\times$[$P_{env} - 0.03$ MPa, P_{env}]) in the two-phase region clinging to the phase envelope, including the critical point. A total of 180,000 points in the test region (with pressure and temperature increments of 50 Pa and 0.1 K, respectively) are employed to perform flash calculations. The performance of different algorithms illustrated based on these points' statistical properties
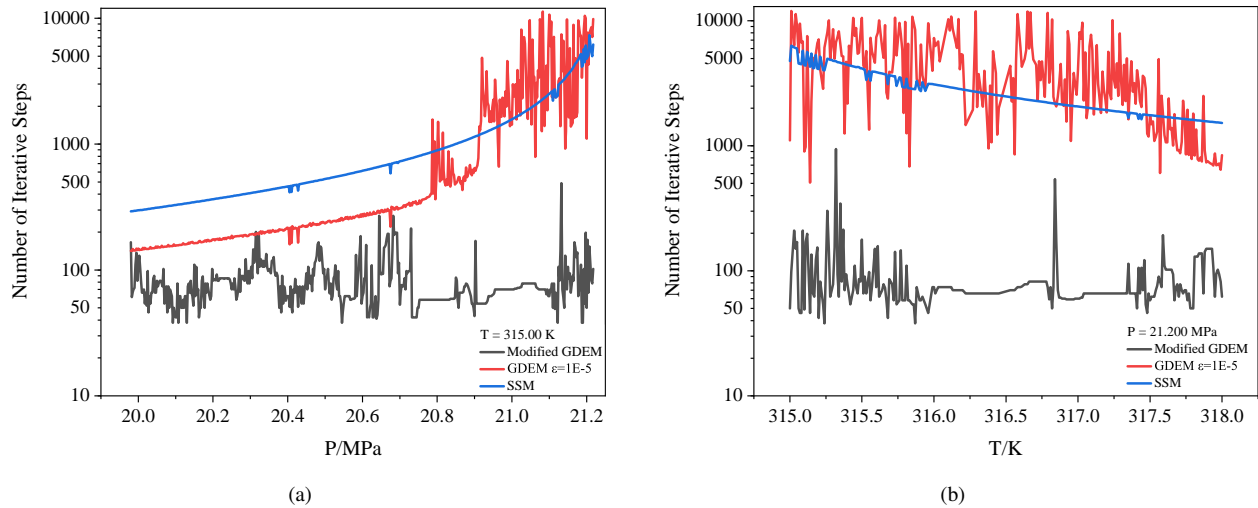
The stability and efficiency of SSM, the conventional GDEM, and the modified GDEM for this flash calculation test are summarized in Table 1. The average iterative steps and CPU times are counted based on the successful test points. Among all the three iterative algorithms, SSM is the most stable, and no flash calculations fail in this test. Accordingly, its efficiency is the lowest.

For the conventional GDEM, since the criterion Eq. (19) is employed to trigger the acceleration process, its stability and efficiency depend on the value of ε. The conservative choice of a small ε seldom fails in flash calculations, but its calculation efficiency is little improved over SSM. Even when ε is set to 10^{-5}, there is still a 14.17% of flash calculation fails in this test. In addition, the calculation efficiency is only approximately 10% better than SSM. Large values of ε improve the computational efficiency significantly, but the stability of the algorithm suffers considerably. In this test, the percentage of failure calculations is 36.81% and 27.95% when ε is set to 10^{-3} and 10^{-4}, respectively. The average number of iterations and the corresponding CPU cost of one successful calculation are not provided in Table 1 for these two cases due to their high failure rates. This test indicates that the conventional GDEM is not efficient for flash calculations near the critical point.

Table 1 shows that the modified GDEM performed well in this test. The stability of the modified GDEM is almost the same as SSM, and only 0.90% of the flash calculations

Fig. 2. Variations of the residuals of fugacity equality for the 9-cp mixture flash calculation test during iterations.

Fig. 3. Number of iterations for the 9-cp mixture flash calculations near the critical point.

fail. In addition, the modified GDEM improves the calculation efficiency greatly. The average number of iterations in the modified GDEM is approximately 1/19 of that in SSM, and the CPU cost is approximately 1/14. Compared to the conventional GDEM with $\varepsilon = 10^{-5}$, a speedup of nearly 12 is reached.
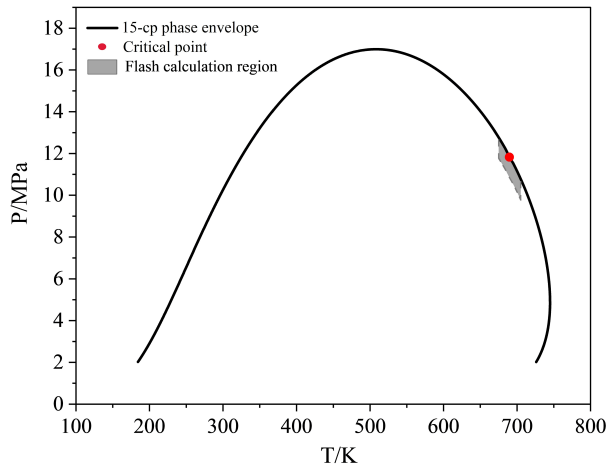
The calculated residuals of fugacity equality during iterations at two specific points ($T = 313.17$ K, $P = 20.800$ MPa and $T = 317.00$ K, $P = 21.174$ MPa) are presented in Fig. 2. Without acceleration, SSM converges smoothly and slowly, but the number of its iterative steps required is the largest, leading to the lowest calculation efficiency. For the conventional GDEM, the number of its iterative steps depends on the choice of the threshold value ε. Larger values of ε can trigger the GDEM acceleration much earlier, and the corresponding number of iterative steps can be significantly reduced from SSM. Applying the criterion Eq. (19) implies that many SSM iterative steps are required before the acceleration process of GDEM is triggered, as mentioned above.

Based on this point, the calculation efficiency cannot be improved much in the conventional GDEM. In contrast, in the modified GDEM, the criterion Eq. (19) is abandoned and replaced by Eq. (24), the post-calibration step; the acceleration is performed immediately after $k + 1$ (normally $k = 3$) steps of SSM iterations. Thus, as shown in Fig. 2, the acceleration operation is triggered the earliest for the modified GDEM, and correspondingly, the fewest iterative steps are required.

Fig. 3 compares the number of iterations required by different algorithms at a fixed temperature of $T = 315.00$ K (see Fig. 3(a)) and a fixed pressure of $P = 21.200$ MPa (see Fig. 3(b)) near the critical point. The number of iterations required in SSM increases notably when the test point approaches the critical point. In Fig. 3(a), the test point moves closer to the critical point as its pressure increases. In Fig. 3(b), the test point moves closer to the critical point as its temperature decreases. The situation is similar for the number of iterations required in the conventional GDEM (with $\varepsilon = 10^{-5}$), though

with fluctuations. In contrast, the number of iterations required in the modified GDEM is stable despite its distance to the critical point. More importantly, of all of the algorithms, the modified GDEM required the least number of iterations, much less than the other two. This test shows that the proposed modified GDEM is much more efficient, especially for flash calculations near the critical point.

Fig. 4. Illustration of the phase envelope and the test region for the 15-cp mixture.
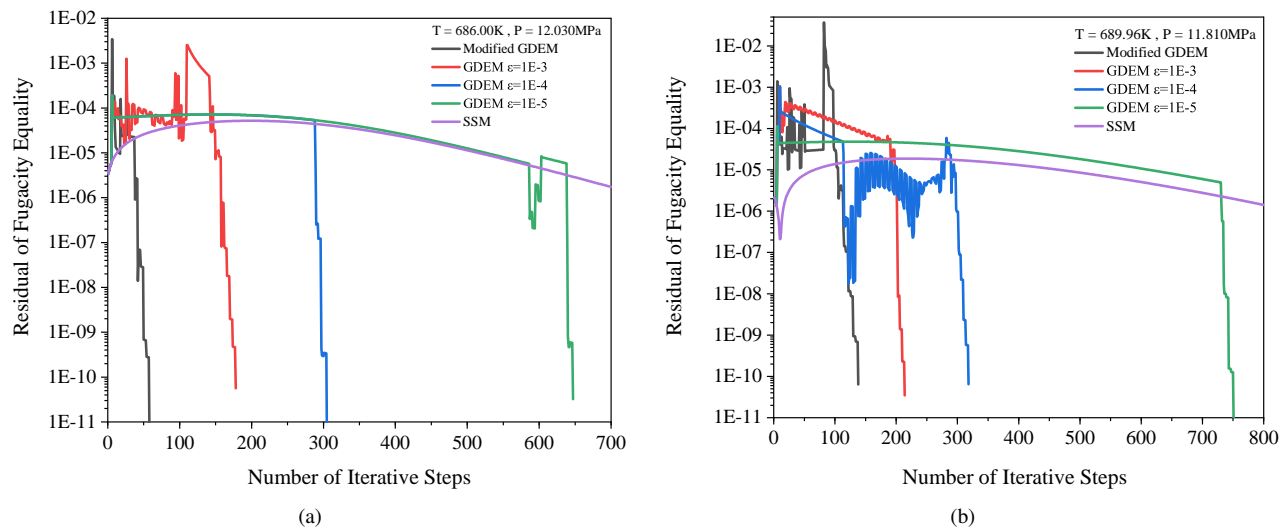
4.2 Test for the 15-component mixture

The 15-component mixture comprises CO_2, N_2, and 13 other hydrocarbons. Fluid compositions and EOS parameters of the 15-component mixture can be found in Hearn and Whitson (1995). Its critical temperature and pressure are $T_c = 689.4$ K and $P_c = 12.20$ MPa. Fig. 4 shows its phase envelope and the test region. The test region is still a curved quadrilateral ($[675$ K, 705 K$] \times [P_{env} - 0.03$ MPa$, P_{env}]$) next to the critical point. A total of 180,000 points in the test region (with pressure and temperature increments of 50 Pa and 0.1 K, respectively) are employed to perform flash calculations.

The stability and efficiency of SSM, the conventional GDEM and the modified GDEM for this flash calculation test are summarized in Table 2. The high stability and efficiency of the proposed modified GDEM are reconfirmed. Only 1.37% of the flash calculations fail for the modified GDEM, indicating its high stability. At the same time, the average number of iterations required in the modified GDEM is approximately 1/25 of that in SSM, and the CPU cost is approximately 1/20, indicating its high efficiency. Even when compared to the conventional GDEM with $\varepsilon = 10^{-5}$, a speedup of nearly 3.5 is reached.
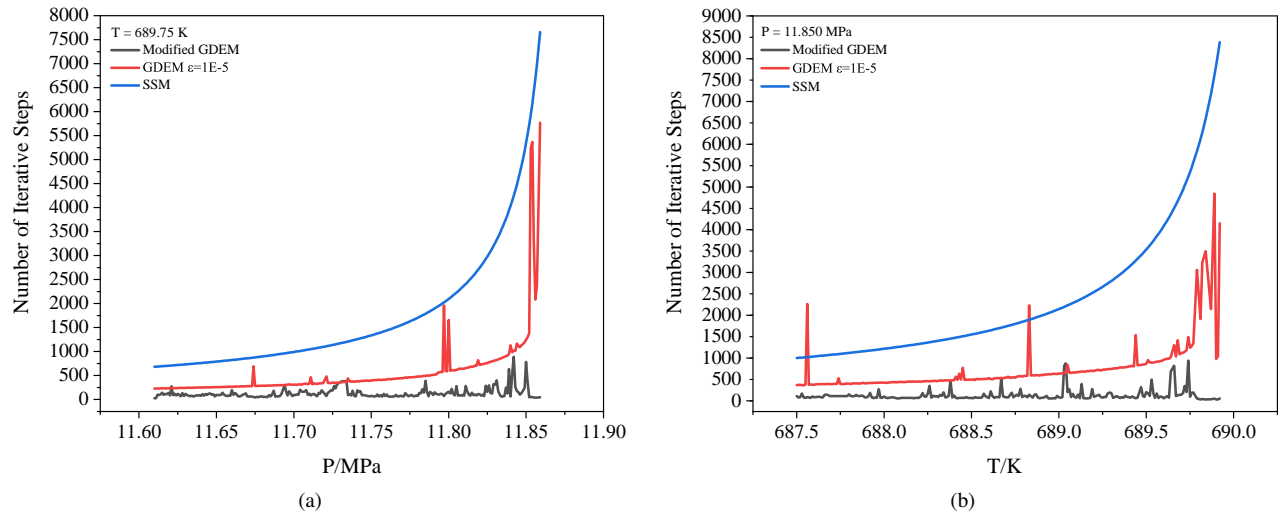
The calculated residuals of fugacity equality during iterations at two specific points ($T = 686.00$ K, $P = 12.030$ MPa and $T = 689.96$ K, $P = 11.810$ MPa) are presented in Fig. 5. It can also be seen that the acceleration operation is triggered the

Table 2. Flash calculation results of the 15-cp mixture.

Algorithm	Failure rate (%)	Average iterative steps	Average CPU time (s)
SSM	0.01	3,402	6.55×10^{-3}
Conventional GDEM (with $\varepsilon = 1.0 \times 10^{-3}$)	22.64	-	-
Conventional GDEM (with $\varepsilon = 1.0 \times 10^{-4}$)	20.03	-	-
Conventional GDEM (with $\varepsilon = 1.0 \times 10^{-5}$)	4.09	690	1.48×10^{-3}
Modified GDEM	1.37	136	3.29×10^{-4}

Fig. 5. Variations of the residuals of fugacity equality for the 15-cp mixture flash calculation test during iterations.

Fig. 6. Number of iterations for the 15-cp mixture flash calculations near the critical point.

Table 3. Flash calculation results of the 28-cp mixture.

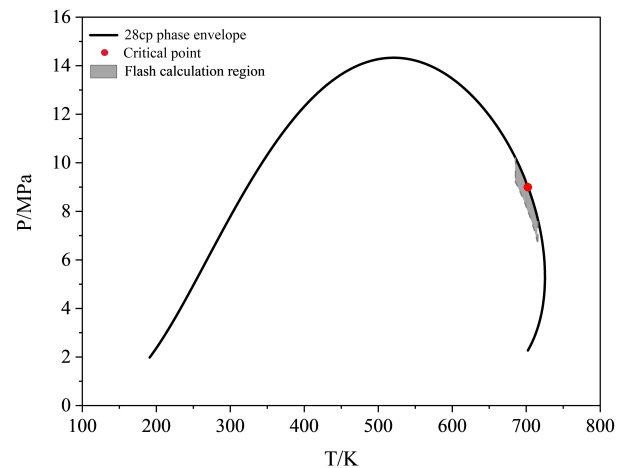| Algorithm	Failure rate (%)	Average iterative steps	Average CPU time (s)
SSM	0.01	2,065	8.65×10^{-3}
Conventional GDEM (with $\varepsilon = 1.0 \times 10^{-3}$)	18.66	-	-
Conventional GDEM (with $\varepsilon = 1.0 \times 10^{-4}$)	17.52	-	-
Conventional GDEM (with $\varepsilon = 1.0 \times 10^{-5}$)	1.98	447	1.99×10^{-3}
Modified GDEM	1.17	113	5.50×10^{-4}

earliest in the modified GDEM. Correspondingly, the required number of iterative steps is the least.

Fig. 6 shows the comparisons among the number of iteration steps required for different algorithms at a fixed temperature of $T = 689.75$ K (see Fig. 6(a)) and a fixed pressure of $P = 11.850$ MPa (see Fig. 6(b)). When approaching the critical point, the number of iterative steps required in SSM and the conventional GDEM increase notably. In contrast, the number of iterations required in the modified GDEM is stable and much smaller than the other two algorithms.

4.3 Test for the 28-component mixture

The 28-component mixture comprises CO_2, N_2, and 26 other hydrocarbons. Fluid compositions and EOS parameters of the 28-component mixture can be found in Hendriks and Van Bergen (1992). Its critical parameters are $T_c = 701.94$ K and $P_c = 9.16$ MPa. Fig. 7 shows the phase envelope of this 28-component mixture and the test region. It is still a curved quadrilateral ([685.00 K, 715.00 K]×[$P_{env} - 0.03$ MPa, P_{env}]) next to the critical point, and a total of 180,000 points in the test region (with pressure and temperature increments of 50 Pa and 0.1 K, respectively) are employed to perform flash calculations.
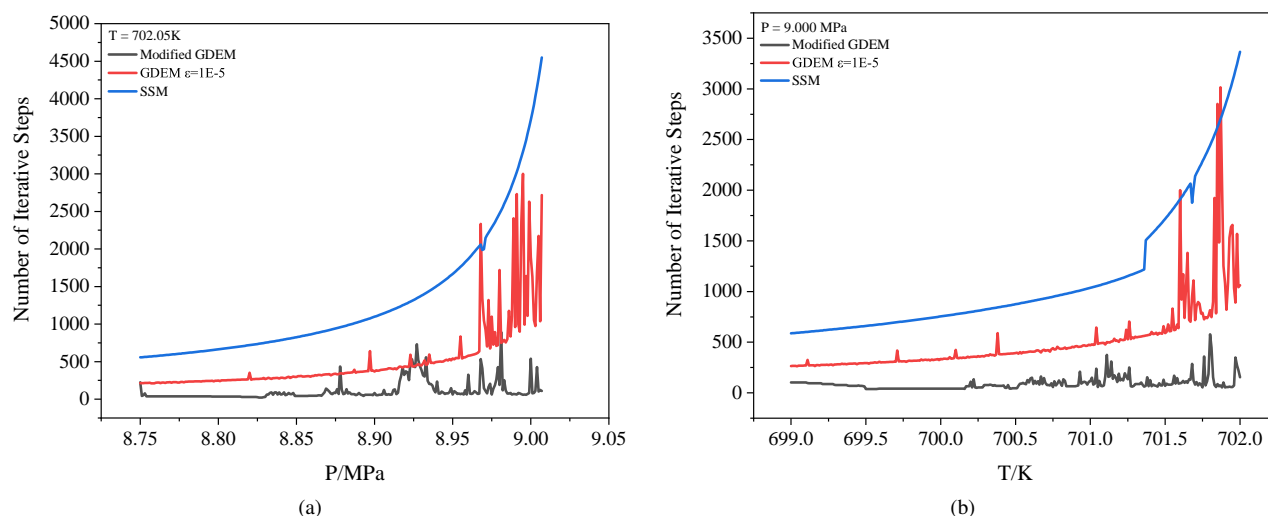
The stability and efficiency of SSM, the conventional GDEM and the modified GDEM for this flash calculation test are summarized in Table 3. The high stability and efficiency

Fig. 7. Illustration of the phase envelope and the test region for the 28-cp mixture.

of the modified GDEM are reconfirmed. Only 1.17% of the flash calculations fail for the modified GDEM in this test. The average number of iterations required in the modified GDEM is approximately 1/18 of that in SSM, and the CPU cost is approximately 1/16. Even when compared to the conventional GDEM with $\varepsilon = 10^{-5}$, a speedup of 2.6 is reached.

The comparisons of the number of iteration steps for different algorithms at a fixed temperature of $T = 702.30$ K (see Fig. 8(a)) and a fixed pressure of $P = 9.000$ MPa (see

Fig. 8. Number of iterations for the 28-cp mixture flash calculations near the critical point.

Fig. 8(b)) are shown in Fig. 8. Near the critical point, the iterative steps of SSM and the conventional GDEM increase rapidly, and the acceleration effect of the conventional GDEM algorithm is unstable. In contrast, the modified GDEM requires fewer iterative steps in the pressure (Fig. 8(a)) and temperature (Fig. 8(b)) areas throughout the test, and the number of iterative steps is maintained at a low level, far less than the iterative steps required by the other two algorithms.

5. Conclusions

Fast and stable flash calculations are crucial in compositional reservoir models. However, flash calculations in the near-critical region of hydrocarbon mixtures can be time-consuming and prone to failure. In this article, a modified GDEM is proposed to improve the speed and stability of flash calculations in the near-critical region. The conclusions are summarized below.

1) The impact of the liquid fraction on the iterative process should be fully taken into consideration. By adding the liquid fraction as a variable when performing GDEM acceleration, the stability of GDEM is greatly improved.

2) A post-calibration step is proposed to replace the conventional criterion. Applying the post-calibration step can ensure the stability of GDEM and improve its efficiency in flash calculations.

3) Numerical tests show that the modified GDEM performs significantly better than SSM and the conventional GDEM. Its stability is almost the same as SSM, which is seen as the most stable algorithm. The calculation efficiency of the modified GDEM remains almost unchanged in the near-critical region and is much higher than SSM and the conventional GDEM.

Acknowledgement

Conflict of interest

The authors declare no competing interest.

References

Afanasyev, A., Andreeva, A., Chernova, A. Numerical optimisation of CO_2 flooding using a hierarchy of reservoir models. Advances in Geosciences, 2021, 56: 19-31.

Belkadi, A., Yan, W., Moggia, E., et al. Speeding up compositional reservoir simulation through an efficient implementation of phase equilibrium calculation. Paper SPE 163598 Presented at SPE Reservoir Simulation Symposium, The Woodlands, Texas, 18-20 February, 2013.

Coats, K. H. An equation of state compositional model. Society of Petroleum Engineers Journal, 1980, 20(5): 363-376.

Coats, K. H. A note on IMPES and some IMPES-based simulation models. SPE Journal, 2000, 5(3): 245-251.

Gorucu, S. E., Johns, R. T. Comparison of reduced and conventional two-phase flash calculations. SPE Journal, 2015, 20(2): 294-305.

Crowe, C., Nishio, M. Convergence promotion in the simulation of chemical processes—the general dominant eigenvalue method. AIChE Journal, 1975, 21(3): 528-533.

Gupta, A. K., Bishnoi, P., Kalogerakis, N. An accelerated successive substitution method for single stage flash calculations. The Canadian Journal of Chemical Engineering, 1988, 66(2): 291-296.

Haugen, K. B., Beckner, B. L. Highly optimized phase equilibrium calculations. Paper SPE 163583 presented at the SPE Reservoir Simulation Symposium, The Woodlands, Texas, 18–20 February, 2013.

Hearn, C. L., Whitson, C. H. Evaluating miscible and im-

miscible gas injection in the safah field, Oman. Paper SPE 29115 presented at the SPE Reservoir Simulation Symposium, San Antonio, Texas, 12–15 February, 1995.

Hendriks, E. M., Van Bergen, A. Application of a reduction method to phase equilibria calculations. Fluid Phase Equilibria, 1992, 74: 17-34.

Hu, X., Wang, M., Shi, A., et al. A modified sequential method for solving the full composition model innumerical reservoir simulation. IOP Conference Series: Materials Science and Engineering, 2020, 782(4): 042054.

Kenyon, D. Third SPE comparative solution project: Gas cycling of retrograde condensate reservoirs. Journal of Petroleum Technology, 1987, 39(8): 981-997.

Li, H. Multiphase Equilibria of Complex Reservoir Fluids: An Equation of State Modeling Approach. Berlin, Germany, Springer Nature, 2021.

Li, Y., Johns, R. T. Rapid flash calculations for compositional simulation. SPE Reservoir Evaluation and Engineering, 2006, 9(5): 521-529.

Li, Z., Firoozabadi, A. General strategy for stability testing and phase-split calculation in two and three phases. SPE Journal, 2012, 17(4): 1096-1107.

Lian, P., Ji, B., Duan, T., et al. Parallel numerical simulation for a super large-scale compositional reservoir. Advances in Geo-Energy Research, 2019, 3(4): 381-386.

Mehra, R., Heidemann, R., Aziz, K. An accelerated successive substitution algorithm. The Canadian Journal of Chemical Engineering, 1983, 61(4): 590-596.

Michelsen, M. Phase equilibrium calculations. What is easy and what is difficult? Computers and Chemical Engineering, 1993, 17(5-6): 431-439.

Michelsen, M. L. The isothermal flash problem. Part I. Stability. Fluid Phase Equilibria, 1982a, 9(1): 1-19.

Michelsen, M. L. The isothermal flash problem. Part II. Phase-split calculation. Fluid Phase Equilibria, 1982b, 9(1): 21-40.

Michelsen, M. L. Simplified flash calculations for cubic equations of state. Industrial and Engineering Chemistry Process Design and Development, 1986, 25(1): 184-188.

Michelsen, M. L., Yan, W., Stenby, E. H. A comparative study of reduced-variables-based flash and conventional flash. SPE Journal, 2013, 18(5): 952-959.

Moncorgé, A., Møyner, O., Tchelepi, H. A., et al. Consistent upwinding for sequential fully implicit multiscale compositional simulation. Computational Geosciences, 2020, 24(2): 533-550.

Moortgat, J. Adaptive implicit finite element methods for multicomponent compressible flow in heterogeneous and fractured porous media. Water Resources Research, 2017, 53(1): 73-92.

Mostafavi, S. E., Khodapanah, E., Tabatabaei-Nezhad, S. A. Development of a fast EoS based compositional model for three-phase core flooding. SN Applied Sciences, 2020, 2(1): 44.

Nichita, D. V., Graciaa, A. A new reduction method for phase equilibrium calculations. Fluid Phase Equilibria, 2011, 302(1-2): 226-233.

Nichita, D. V., Leibovici, C. F. A rapid and robust method for solving the Rachford–Rice equation using convex transformations. Fluid Phase Equilibria, 2013, 353: 38-49.

Orbach, O., Crowe, C. Convergence promotion in the simulation of chemical processes with recycle-the dominant eigenvalue method. The Canadian Journal of Chemical Engineering, 1971, 49(4): 509-513.

Pan, H., Firoozabadi, A. Fast and Robust Algorithm for Compositional Modeling: Part II–Two-Phase Flash Computations. SPE Journal, 2003, 8(4): 380-391

Peng, D. -Y., Robinson, D. B. A new two-constant equation of state. Industrial and Engineering Chemistry Fundamentals, 1976, 15(1): 59-64.

Petitfrere, M., Nichita, D. V. A comparison of conventional and reduction approaches for phase equilibrium calculations. Fluid Phase Equilibria, 2015, 386: 30-46.

Rachford, H. H., Rice, J. Procedure for use of electronic digital computers in calculating flash vaporization hydrocarbon equilibrium. Journal of Petroleum Technology, 1952, 4(10): 19-13.

Soave, G. Equilibrium constants from a modified Redlich-Kwong equation of state. Chemical Engineering Science, 1972, 27(6): 1197-1203.

Soeder, D. J. Greenhouse gas sources and mitigation strategies from a geosciences perspective. Advances in Geo-Energy Research, 2021, 5(3): 274-285.

Soliman, M. A modified general dominant eigenvalue method for convergence acceleration of cyclic systems. The Canadian Journal of Chemical Engineering, 1981, 59(3): 395-397.

Soliman, M. A. On the convergence acceleration of iterative processes. Computers and Chemical Engineering, 1985, 9(1): 97-98.

Wang, S., Yuan, D., Winterfeld, P. H., et al. Understanding the multiphysical processes in CO_2-EOR operations: A numerical study using a general simulation framework. SPE Journal, 2021, 26(2): 918-939.

Wegstein, J. H. Accelerating convergence of iterative processes. Communications of the ACM, 1958, 1(6): 9-13.

Xu, T., Tian, H., Zhu, H., et al. China actively promotes CO_2 capture, utilization and storage research to achieve carbon peak and carbon neutrality. Advances in Geo-Energy Research, 2022, 6(1): 1-3

Zhao, H., Jing, H., Fang, Z., et al. Flash calculation using successive substitution accelerated by the general dominant eigenvalue method in reduced-variable space: Comparison and new insights. SPE Journal, 2020, 25(6): 3332-3348.

Zhu, D., Eghbali, S., Shekhar, C., et al. A unified algorithm for phase-stability/split calculation for multiphase isobaric-isothermal flash. SPE Journal, 2018, 23(2): 498-521.